

Single-channel or multichannel thermal transport: Effect of higher-order anharmonic corrections on the predicted phonon thermal transport properties of semiconductors

Ankit Jain*

Mechanical Engineering Department, IIT Bombay, Powai, Mumbai, Maharashtra 400076, India
 (Received 27 January 2022; revised 20 May 2022; accepted 14 July 2022; published 27 July 2022)

The phonon thermal transport properties of eight ternary intermetallic semiconductors are investigated by accounting for higher-order four-phonon scattering, phonon renormalization, and multichannel thermal transport. The commonly used lowest-order theory, which accounts only for three-phonon scattering and without phonon renormalization, fails drastically for the considered materials and underpredicts the thermal conductivity by up to a factor of two. The thermal conductivity decreases for three compounds and increases for five compounds with the application of higher-order corrections owing to a contrasting role of four-phonon scattering and phonon stiffening on the predicted thermal conductivity. Using the higher-order theory, at a temperature of 300 K, the lowest obtained thermal conductivity is 0.31 W/m K for BiCsK₂ and three other compounds (SbCsK₂, SbRbNa₂, and SbRbK₂) have thermal conductivities lower than 0.5 W/m K via the particlelike phonon transport channel. The contribution from the wavelike coherent transport channel is lower than 0.05 W/m K in all of these ultralow thermal conductivity compounds. The higher-order theory is crucial for the correct description of thermal transport physics, failing which the thermal transport is wrongly characterized as multichannel transport by the lowest-order theory.

DOI: [10.1103/PhysRevB.106.045207](https://doi.org/10.1103/PhysRevB.106.045207)

I. INTRODUCTION

With advances in computational resources in the past decade, it is now possible to predict the phonon thermal conductivity of semiconducting crystalline materials by solving the Boltzmann transport equation (BTE) with inputs from *ab initio* calculations [1–4]. The BTE theory accounts only for three-phonon interactions at the lowest order [4–6]. While this lowest-order theory is found to work well for relatively simple materials and an excellent agreement with experiments is obtained wherever possible [3,6,7], recently, this theory has been reported to fail severely for several low and high thermal conductivity compounds (such as BAs [8], Tl₃VSe₄ [9], MoS₂ [10]). In particular, it is shown that (a) phonon scattering due to higher-order four-phonon processes and (b) phonon renormalization due to quartic anharmonicity are significant in these technologically relevant materials not accounted for in the lowest-order theory [11–14]. For binary compounds with a zinc-blende crystal structure, applying the first of these corrections resulted in an up to 75% reduction in thermal conductivity at room temperature [14]. For Tl₃VSe₄, on the other hand, these higher-order corrections resulted in more than a factor of two increase in the thermal conductivity [9,13]. In comparison to the lowest-order theory, the higher-order corrections are three to four orders of magnitude expensive to compute and their application is currently limited to a handful of materials [9,11–14].

In parallel, the failure of the lowest-order transport theory to describe the experimentally measured thermal transport in

ultralow thermal conductivity solids has also motivated the development of several heuristics-based multichannel thermal transport models where on top of the particlelike phonon transport channel, an additional contribution arising from diffusionlike heat transfer channel is taken into account to explain the underprediction of experimentally measured values [15,16]. These developments subsequently evolved into a derivation of unified thermal transport theory capable of describing the thermal transport in the spectrum of materials varying from purely amorphous to perfectly crystalline solids [17]. The major finding of this unified thermal transport theory is the contribution from both particlelike (originating from well-defined phonon modes) and wavelike (from tunneling/coherence between modes) transport channels towards the thermal transport. In practical implementations, the unified/multichannel thermal transport theory requires phonon mode properties (frequency, linewidth, etc.) which can be obtained by either using only the lowest-order theory or by also including the higher-order corrections. Since higher-order corrections are computationally demanding, the application of multichannel thermal transport in the literature is extremely limited to lowest-order theory driven phonon properties and its validity/significance is debated when higher-order corrections are taken into account [13].

In this regard, the phonon thermal transport of eight ternary semiconducting compounds with stoichiometry ABC_2 [$A \in (\text{Sb, Bi})$, $B \in (\text{Na, K, Rb, Cs})$, and $C \in (\text{Li, Na, K})$] is investigated in this paper by employing the higher-order corrections and unified thermal transport theory. At a temperature of 300 K, the thermal conductivity of these compounds varies between 0.16 and 6.1 W/m K using the lowest-order theory. The combined effect of four-phonon scattering and

*a_jain@iitb.ac.in

phonon renormalization resulted in a decrease in thermal conductivity for three of the considered compounds and an increase in thermal conductivity for five considered compounds. The maximum change in thermal conductivity is for SbRbK₂, for which the thermal conductivity increases by more than a factor of two (from 0.16 to 0.37 W/m K) with the inclusion of these corrections. The particlelike single-channel phonon transport picture is erroneously invalid at the lowest order of theory and the application of higher-order corrections results in a single-channel thermal transport with a coherent channel contribution of less than 13% in all of the considered compounds.

II. METHODOLOGY

The contribution of a particlelike phonon transport channel towards the thermal transport in the α direction is obtained by solving the Boltzmann transport equation and the Fourier's law, as [18,19]

$$k_{\alpha}^p = \sum_{\lambda} c_{\lambda} v_{\lambda,\alpha}^2 \tau_{\lambda,\alpha}, \quad (1)$$

where k_{α}^p represents the thermal conductivity, the summation is over all the phonon wave vectors \mathbf{q} and polarizations ν enumerated by a composite index $\lambda = (\mathbf{q}, \nu)$, c_{λ} is the phonon specific heat, $v_{\lambda,\alpha}$ is the α component of the phonon group velocity vector \mathbf{v}_{λ} , and $\tau_{\lambda,\alpha}$ is the phonon scattering time. The phonon specific heat is obtained from the phonon vibrational frequencies as $c_{\lambda} = \frac{\hbar\omega_{\lambda}}{V} \frac{\partial n_{\lambda}^o}{\partial T}$, where n_{λ}^o , \hbar , ω_{λ} , V , and

T are the Bose-Einstein distribution, reduced Planck constant, phonon frequency, crystal volume, and temperature. The phonon group velocities can be obtained as $\mathbf{v}_{\lambda} = \frac{\partial\omega_{\lambda}}{\partial\mathbf{q}}$ and the phonon frequencies are obtained from the diagonalization of the dynamical matrix as $\omega_{\lambda}^2 \mathbf{e}_{\lambda} = \mathbf{D}_{\mathbf{q}} \cdot \mathbf{e}_{\lambda}$, where \mathbf{e}_{λ} is the eigenvector and $\mathbf{D}_{\mathbf{q}}$ is the dynamical matrix whose elements $D_{\mathbf{q}}^{3(b-1)+\alpha,3(b'-1)+\beta}$ are given by

$$D_{\mathbf{q}}^{3(b-1)+\alpha,3(b'-1)+\beta} = \sum_l \frac{\Phi_{b0;b'l'}^{\alpha\beta}}{\sqrt{m_b m_{b'}}} e^{i\mathbf{q}\cdot(\mathbf{r}_{b'l'} - \mathbf{r}_{b0})}, \quad (2)$$

with the summation running over all unit cells in the lattice (N), and m_b, \mathbf{r}_{bl} being the mass and position vector of atom b in the l th unit cell, and $\Phi_{ij}^{\alpha\beta}$ is the real-space ($ij, \alpha\beta$) element of the harmonic force constant matrix Φ .

At the lowest level of theory, the Φ used in Eq. (2) is a bare-harmonic force constant (as obtained from finite-difference or density functional perturbation theory and without renormalization). The phonon-phonon scattering rates at the lowest order of theory are limited to three-phonon processes and are obtained as [9,18,20,21]

$$\frac{1}{\tau_{\lambda}^{3ph}} = \sum_{\lambda_1, \lambda_2} \left\{ (n_{\lambda_1} - n_{\lambda_2}) W^+ + \frac{1}{2} (n_{\lambda_1} + n_{\lambda_2} + 1) W^- \right\}, \quad (3)$$

where W represents the scattering probability matrix given by

$$W^{\pm} = \frac{2\pi}{\hbar^2} |\Psi_{\lambda(\pm\lambda_1)(-\lambda_2)}|^2 \delta(\omega_{\lambda} \pm \omega_{\lambda_1} - \omega_{\lambda_2}), \quad (4)$$

$\pm\lambda = (\pm\mathbf{q}, \nu)$, and $\Psi_{\lambda(\lambda_1)(\lambda_2)}$ are the Fourier transforms of real-space cubic constants $\Psi_{bl;b'l';b''l''}^{\alpha\beta\gamma}$, and are obtained as

$$\Psi_{\lambda\lambda_1\lambda_2} = \Psi_{\mathbf{q}\mathbf{q}'\mathbf{q}''}^{\nu\nu'\nu''} = N \left(\frac{\hbar}{2N} \right)^{\frac{3}{2}} \sum_b \sum_{b'l'} \sum_{b''l''} \sum_{\alpha\beta\gamma} \Psi_{bl;b'l';b''l''}^{\alpha\beta\gamma} \frac{\tilde{\epsilon}_{b\lambda}^{\alpha} \tilde{\epsilon}_{b'l'}^{\beta} \tilde{\epsilon}_{b''l''}^{\gamma}}{\sqrt{m_b \omega_{\lambda} m_{b'} \omega_{\lambda'} m_{b''} \omega_{\lambda''}}} e^{i(\mathbf{q}'\cdot\mathbf{r}_{0l'} + \mathbf{q}''\cdot\mathbf{r}_{0l''})}. \quad (5)$$

The δ in Eq. (5) represents the delta function ensuring energy conservation and the summation is performed over phonon wave vectors satisfying crystal momentum conservation, i.e., $\mathbf{q} + \mathbf{q}_1 + \mathbf{q}_2 = \mathbf{G}$, where \mathbf{G} is the reciprocal space lattice vector.

At the higher order of theory, the phonon-phonon scattering rates are obtained by considering both three-phonon and four-phonon processes. The scattering rates of phonons due to second order, i.e., four-phonon processes, are obtained as [9,11,18,22]

$$\frac{1}{\tau_{\lambda}^{4ph}} = \sum_{\lambda_1, \lambda_2, \lambda_3} \left\{ \frac{1}{6} \left\{ \frac{n_{\lambda_1} n_{\lambda_2} n_{\lambda_3}}{n_{\lambda}} W^{--} \right\} + \frac{1}{2} \left\{ \frac{(n_{\lambda_1} + 1) n_{\lambda_2} n_{\lambda_3}}{n_{\lambda}} W^{+-} \right\} + \frac{1}{2} \left\{ \frac{(n_{\lambda_1} + 1)(n_{\lambda_2} + 1) n_{\lambda_3}}{n_{\lambda}} W^{++} \right\} \right\}, \quad (6)$$

where $W^{\pm\pm}$ represents the scattering probability matrix given by

$$W^{\pm\pm} = \frac{2\pi}{\hbar^2} |\Xi_{\lambda(\pm\lambda_1)(\pm\lambda_2)(-\lambda_3)}|^2 \delta(\omega_{\lambda} \pm \omega_{\lambda_1} \pm \omega_{\lambda_2} - \omega_{\lambda_3}), \quad (7)$$

and $\Xi_{\lambda(\lambda_1)(\lambda_2)(\lambda_3)}$ are the Fourier transforms of the quartic force constants $\Xi_{ijkl}^{\alpha\beta\gamma\delta}$, and are obtained as

$$\Xi_{\lambda\lambda_1\lambda_2\lambda_3} = \Xi_{\mathbf{q}\mathbf{q}'\mathbf{q}''\mathbf{q}'''}^{\nu\nu'\nu''\nu'''} = N \left(\frac{\hbar}{2N} \right)^2 \sum_{bb'b'l'} \sum_{l''l'''} \sum_{\alpha\beta\gamma\delta} \Xi_{bl;b'l';b''l'';b'''}^{\alpha\beta\gamma\delta} \frac{\tilde{\epsilon}_{b\lambda}^{\alpha} \tilde{\epsilon}_{b'l'}^{\beta} \tilde{\epsilon}_{b''l''}^{\gamma} \tilde{\epsilon}_{b'''}^{\delta}}{\sqrt{m_b \omega_{\lambda} m_{b'} \omega_{\lambda'} m_{b''} \omega_{\lambda''} m_{b'''} \omega_{\lambda'''}}} e^{i(\mathbf{q}'\cdot\mathbf{r}_{0l'} + \mathbf{q}''\cdot\mathbf{r}_{0l''} + \mathbf{q}'''\cdot\mathbf{r}_{0l'''})}. \quad (8)$$

Similar to Eqs. (4) and (5), the summations in Eq. (8) are performed over phonon wave vectors satisfying crystal momentum conservation and δ ensures energy conservation during the four-phonon scattering event.

Further, at the higher order of theory, the phonon frequencies and eigenvectors are obtained from Eq. (2) using the renormalized harmonic force constants $\Phi_{ij}^{c,\alpha\beta}$, which are obtained as [11,20]

$$\Phi_{ij}^{c,\alpha\beta} = \Phi_{ij}^{o,\alpha\beta} + \frac{\hbar}{4N} \sum_{l''l'''} \sum_{b''b'''} \sum_{\gamma\delta} \sum_{\mathbf{q}\mathbf{v}} \Xi_{ijkl}^{\alpha\beta\gamma\delta} \frac{\tilde{\epsilon}_{b''\lambda}^{\gamma} \tilde{\epsilon}_{b'''}^{\delta}}{\omega_{\lambda} \sqrt{m_{b''} m_{b'''}}} (2n_{\lambda} + 1) e^{i\mathbf{q}\cdot(\mathbf{r}_{0l''} - \mathbf{r}_{0l'''})}, \quad (9)$$

where $\Phi_{ij}^{o,\alpha\beta}$ represent the raw harmonic force constants (as obtained from *ab initio* calculations).

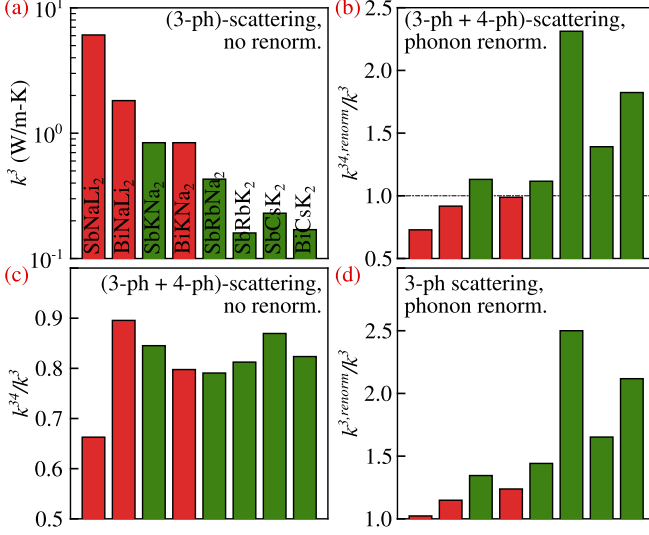


FIG. 1. The thermal conductivity of considered compounds at 300 K as obtained by considering (a) lowest-order theory k^3 , and (b) higher-order four-phonon scattering and quartic renormalization corrections $k^{34,renorm}$. The relative importance of (c) four-phonon scattering k^{34}/k^3 and (d) quartic renormalization $k^{3,renorm}/k^3$ on the predicted thermal conductivity. The materials for which thermal conductivity increases (decreases) with higher-order theory are colored green (red).

Finally, to account for multichannel thermal transport, the contribution of the coherent channel k_α^c can be obtained using the off-diagonal terms of the velocity operator as [17]

$$k_\alpha^c = \frac{\hbar^2}{k_B T^2} \frac{1}{VN} \sum_q \sum_{(v \neq v_1)} \frac{\omega_{qv} + \omega_{qv_1}}{2} V_{q,vv_1}^\alpha V_{q,v_1v}^\alpha \times \frac{\omega_{qv} n_{qv} (n_{qv} + 1) + \omega_{qv_1} n_{qv_1} (n_{qv_1} + 1)}{4(\omega_{qv} - \omega_{qv_1})^2 + (\Gamma_{qv} + \Gamma_{qv_1})^2} (\Gamma_{qv} + \Gamma_{qv_1}), \quad (10)$$

where Γ_{qv} is the phonon linewidth ($\Gamma_{qv} = 1/\tau_{qv}$) and V_{q,vv_1}^α is the α component of the velocity operator and can be obtained as

$$V_{q,vv_1} = \frac{1}{2\sqrt{\omega_{qv}\omega_{qv_1}}} \langle e_{qv} | \frac{\partial D_q}{\partial q} | e_{qv_1} \rangle, \quad (11)$$

using the Wallace/smooth representation of the dynamical matrix [Eq. (2)] [23]. Further details on these methods are available in Refs. [9,21,24–26]. The computational details and the convergence of predicted results with the choice of numerical parameters are reported in Secs. S1–S3 in the Supplemental Material (SM) [27].

III. RESULTS

By considering only the particlelike transport channel, at a temperature of 300 K, the thermal conductivities of the considered compounds vary between 0.16 and 6.08 W/m K using the lowest-order theory as reported in Fig. 1(a). On inclusion of higher-order corrections in Fig. 1(b), the thermal conductivity decreases for three compounds and increases for five

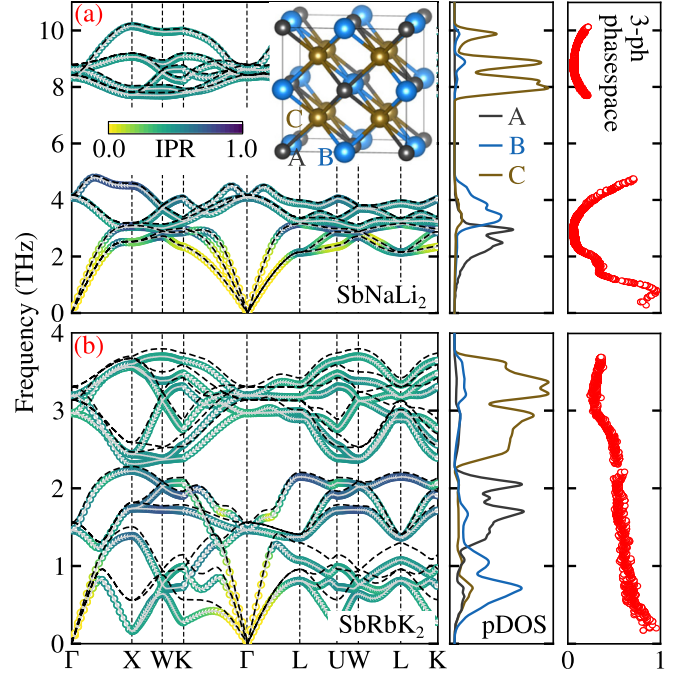


FIG. 2. The representative phonon dispersion of materials with (a) frequency band gaps and (b) weakly bonded atoms. The gray solid and black dashed lines represent nonrenormalized and renormalized (at 300 K) results. The markers are colored according to the inverse participation ratio of modes which varies between 0 and 1 for localized and delocalized modes.

compounds. The maximum decrease (increase) is for SbNaLi₂ (SbRbK₂), for which thermal conductivity decreases by 27% (increases by more than a factor of two) with the inclusion of higher-order corrections. To understand the origin of this puzzling role of higher-order corrections on the predicted thermal conductivity, the effects of four-phonon scattering and phonon renormalization are considered separately.

Compared to the lowest-order theory, the inclusion of four-phonon scattering processes decreases the thermal conductivity for all considered compounds due to an additional phonon scattering channel. The extent to which the phonon thermal conductivity is affected depends on two factors: (i) how much was three-phonon scattering to start with and (ii) how strong is four-phonon scattering. The extent of three-phonon scattering, in turn, is dependent on the number of three-phonon processes which are able to satisfy the scattering selection rules and the strength of each of these scattering processes. The number of three-phonon processes which can satisfy the crystal momentum and energy conservation selection rules can be obtained from the phonon spectrum and are characterizable using the three-phonon scattering phase space (see Fig. 2). For instance, among the two representative phonon spectra presented in Fig. 2, the presence of frequency gaps in the spectrum of SbNaLi₂ makes it difficult to satisfy the energy conservation selection rule (see details in Sec. S3) and results in the reduction of three-phonon scattering phase space (to almost zero) for several mid- and high-frequency optical phonons. This nonscattering of optical phonons via three-phonon processes gets reflected in their high

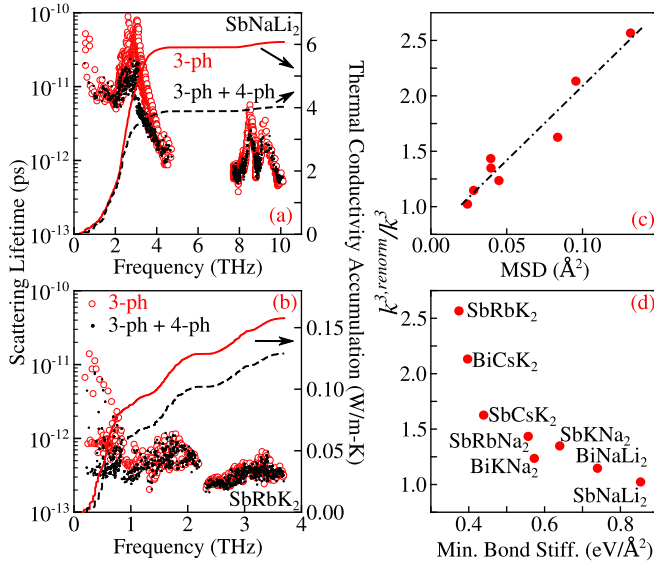


FIG. 3. The phonon scattering lifetimes obtained by considering only three-phonon scattering and by considering both three- and four-phonon scattering for (a) SbNaLi_2 and (b) SbRbK_2 . The thermal conductivity enhancement of considered compounds with phonon renormalization plotted against (c) thermal MSD and (d) effective bond stiffness. The reported MSDs (bond stiffness) in (c) [(d)] are the maximum (minimum) of all atoms in a considered compound. Note that the phonon scattering lifetimes are obtained without considering phonon renormalization in (a) and (b). The scattering lifetimes obtained by including phonon renormalization are reported in Fig. S5 for SbRbK_2 .

contribution to thermal transport at the lowest order of theory. With the inclusion of higher-order four-phonon scattering, these otherwise unscattered phonons are able to undergo scattering which results in their reduced contribution to thermal transport [28]. In the particular case of SbNaLi_2 at 300 K, the contribution of mid-frequency optical phonons (2–4 THz) is reduced from 4.3 to 2.4 W/mK with the inclusion of four-phonon scattering [Fig. 3(a)], which corresponds to a 34% reduction in the total predicted thermal conductivity.

The strength of the individual three-phonon and four-phonon scattering processes depends on the anharmonicity experienced by the atoms. For materials with strongly bonded atoms, the atoms move very little around their equilibrium positions and are limited to the harmonic part of the potential energy surface. In contrast, for materials with weakly bonded atoms, the atoms are able to move far away from their equilibrium positions and experience the more anharmonic part of the potential energy surface. In such materials, the effect of four-phonon scattering is strongest on modes dominated by loosely bound atoms (which happen to be the heat-carrying acoustic modes). For instance, in SbRbK_2 , the acoustic modes are dominated by weakly bonded Rb atoms [29] and have frequencies up to 1.5 THz. In contrast, for SbNaLi_2 , the corresponding modes have a contribution from strongly bonded Sb atoms and have frequencies up to 2.5 THz. As a result, while the contribution of sub-THz modes reduces by 29% with the inclusion of four-phonon scattering in SbRbK_2 , the

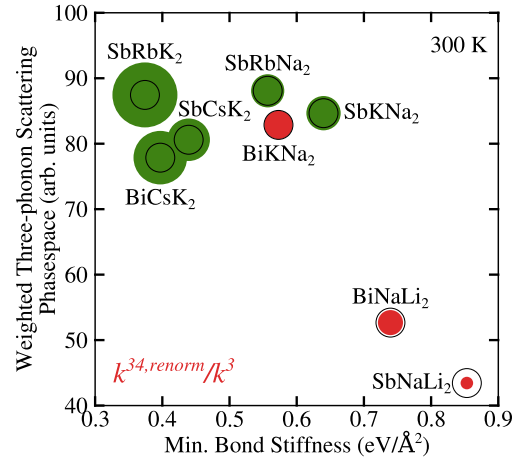


FIG. 4. The change in thermal conductivity of considered compounds with higher-order corrections as summarized using bond stiffness and scattering phase space. The materials for which thermal conductivity decreases (increases) with higher-order corrections are highlighted using red (green) circles. The size of the circles is proportional to the fractional change in thermal conductivity and black circles represent no change in thermal conductivity.

corresponding reduction is less than 8% for modes with frequencies up to 2 THz in SbNaLi_2 [Fig. 3(b)].

With phonon renormalization, the heat-carrying acoustic phonons become stiff in all considered materials, resulting in an increase in the predicted thermal conductivity [Fig. 1(d)]. The extent of renormalization is proportional to (a) the thermal mean square displacement (MSD) of atoms and (b) the strength of the quartic force constant [Eq. (9)]. The strength of the quartic force constants or anharmonicity is, in general, dependent on atomic displacements around their equilibrium positions (not true for perfectly harmonic ideal crystals). As such, the enhancement in thermal conductivity with renormalization is expected to have a strong dependence on thermal MSD. This is reported in Fig. 3(d) where a linear dependence is obtained between the thermal conductivity enhancement and MSDs. Since large MSDs are a manifestation of weak atomic bonding, the thermal conductivity enhancement also correlates strongly with the effective bond stiffness [Fig. 3(d)] [30].

Now that it is established that the three-phonon scattering phase space and effective bond stiffness are instrumental in describing the individual effects of four-phonon scattering and phonon renormalization, the otherwise puzzling thermal conductivity data of Fig. 1(b) is replotted in Fig. 4 as a function of two simple material descriptors, namely, weighted three-phonon scattering phase space and effective bond stiffness. The weighted three-phonon scattering phase space $\bar{\gamma}$ is obtained as $\bar{\gamma} = \frac{\sum_q \sum_\nu c_{q\nu} v_{q\nu, \alpha}^2 \gamma_{q\nu}}{\sum_q \sum_\nu c_{q\nu} v_{q\nu, \alpha}^2}$, where $\gamma_{q\nu}$ represents the scattering phase space of mode $q\nu$. As can be seen from Fig. 4, these descriptors are able to characterize the role of higher-order theory on the predicted thermal conductivity and suggest that (i) for materials with weak interatomic bonding, the thermal conductivity increases with higher-order corrections, (ii) for materials with reduced three-phonon scattering phase space, the thermal conductivity decreases with

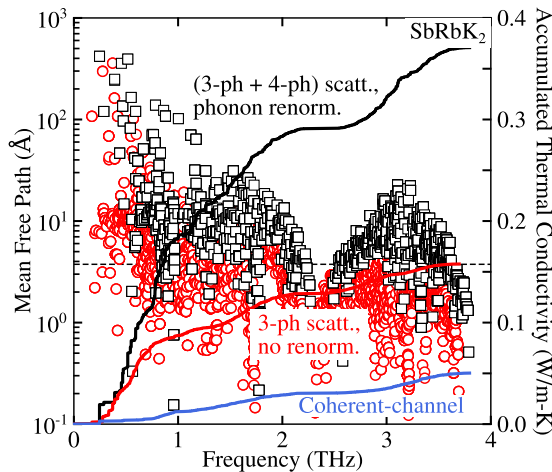


FIG. 5. The mode-dependent contribution to thermal conductivity of SbRbK_2 from particlelike phonon (red and black lines) and wavelike coherent (purple line) transport channels. The red and black data sets correspond to results obtained using the lowest-order theory and higher-order theory. The dashed horizontal line represents the Ioffe-Regel limit [31,32].

higher-order corrections, and (iii) for materials with stiff bonds and high three-phonon scattering phase space, there is no significant change in thermal conductivity. As such, these simple (based on bare harmonic properties) and yet powerful descriptions can be used for the accelerated discovery/screening of ultralow thermal conductivity materials without requiring computationally expensive calculations.

Using the lowest-order transport theory, the predicted thermal conductivity of two compounds is lower than 0.2 W/m K at a temperature of 300 K which is comparable to the reported lowest thermal conductivity of solids in literature [9,15,21]. For such low thermal conductivity materials, the phonon mean free paths could become shorter than the Ioffe-Regel limit, and in such cases, an additional contribution from the wavelike coherent transport channel becomes significant towards the thermal transport [15,17,31]. To check for this, the

phonon mean free paths are compared against the Ioffe-Regel limit [32] for the lowest thermal conductivity (as obtained from the lowest-order theory) compound in Fig. 5.

As can be seen from Fig. 5, while the phonon mean free paths are shorter than the Ioffe-Regel limit for the majority of the phonons using the lowest-order theory, the mean free paths increase to values larger than the Ioffe-Regel limit on the inclusion of higher-order corrections. As such, the particlelike phonon picture is valid for the majority of the phonons and the contribution of the wavelike coherent transport channel is minimal (less than 13% for SbRbK_2 using the higher-order theory as opposed to more than 30% using the lowest-order theory). This validity of the particlelike phonon picture on the incorporation of higher-order corrections and its failure at the lowest order of theory highlights the importance of describing correct phonon properties in multichannel transport models to correctly capture the underlying thermal transport physics.

IV. CONCLUSIONS

In summary, by investigating the thermal transport in eight ternary semiconducting solids using the higher-order transport theory, the weighted three-phonon scattering phase space and effective bond stiffness are identified as simple material descriptors to characterize the puzzling role of higher-order four-phonon scattering and phonon renormalization on the predicted thermal conductivity of materials. The higher-order corrections are essential for the correct description of thermal transport physics in ultralow thermal conductivity solids and the use of the lowest-order theory erroneously suggests multichannel thermal transport in such materials.

ACKNOWLEDGMENTS

The author acknowledges the financial support from IRCC-IIT Bombay and the National Supercomputing Mission, Government of India (Grant No. DST/NSM/R&D-HPC-Applications/2021/10). The calculations are carried out on SpaceTime-II supercomputing facility of IIT Bombay and PARAM Sanganak supercomputing facility of IIT Kanpur.

- [1] K. Esfarjani and H. T. Stokes, *Phys. Rev. B* **77**, 144112 (2008).
- [2] K. Esfarjani, G. Chen, and H. T. Stokes, *Phys. Rev. B* **84**, 085204 (2011).
- [3] L. Lindsay, C. Hua, X. Ruan, and S. Lee, *Mater. Today Phys.* **7**, 106 (2018).
- [4] A. J. McGaughey, A. Jain, H.-Y. Kim, and B. Fu, *J. Appl. Phys.* **125**, 011101 (2019).
- [5] L. Lindsay, D. A. Broido, and T. L. Reinecke, *Phys. Rev. Lett.* **111**, 025901 (2013).
- [6] L. Lindsay, D. A. Broido, and T. L. Reinecke, *Phys. Rev. B* **87**, 165201 (2013).
- [7] A. Jain and A. J. McGaughey, *Comput. Mater. Sci.* **110**, 115 (2015).
- [8] K. Chen, B. Song, N. K. Ravichandran, Q. Zheng, X. Chen, H. Lee, H. Sun, S. Li, G. A. G. U. Gamage, F. Tian *et al.*, *Science* **367**, 555 (2020).
- [9] A. Jain, *Phys. Rev. B* **102**, 201201(R) (2020).
- [10] A. G. Gokhale, D. Visaria, and A. Jain, *Phys. Rev. B* **104**, 115403 (2021).
- [11] N. K. Ravichandran and D. Broido, *Phys. Rev. B* **98**, 085205 (2018).
- [12] T. Feng and X. Ruan, *Phys. Rev. B* **97**, 045202 (2018).
- [13] Y. Xia, K. Pal, J. He, V. Ozoliņš, and C. Wolverton, *Phys. Rev. Lett.* **124**, 065901 (2020).
- [14] N. K. Ravichandran and D. Broido, *Phys. Rev. X* **10**, 021063 (2020).
- [15] S. Mukhopadhyay, D. S. Parker, B. C. Sales, A. A. Puretzky, M. A. McGuire, and L. Lindsay, *Science* **360**, 1455 (2018).
- [16] Y. Luo, X. Yang, T. Feng, J. Wang, and X. Ruan, *Nat. Commun.* **11**, 2554 (2020).
- [17] M. Simoncelli, N. Marzari, and F. Mauri, *Nat. Phys.* **15**, 809 (2019).
- [18] J. A. Reissland, *The Physics of Phonons* (Wiley, New York, 1973).

- [19] M. T. Dove, *Introduction to Lattice Dynamics* (Cambridge University Press, Cambridge, UK, 1993).
- [20] D. C. Wallace, *Thermodynamics of Crystals* (Cambridge University Press, Cambridge, UK, 1972).
- [21] S. Godse, Y. Srivastava, and A. Jain, *J. Phys.: Condens. Matter* **34**, 145701 (2022).
- [22] T. Feng, L. Lindsay, and X. Ruan, *Phys. Rev. B* **96**, 161201(R) (2017).
- [23] M. Simoncelli, N. Marzari, and F. Mauri, [arXiv:2112.06897](https://arxiv.org/abs/2112.06897).
- [24] P. Giannozzi, S. Baroni, N. Bonini, M. Calandra, R. Car, C. Cavazzoni, D. Ceresoli, G. L. Chiarotti, M. Cococcioni, I. Dabo, A. D. Corso, S. de Gironcoli, S. Fabris, G. Fratesi, R. Gebauer, U. Gerstmann, C. Gougoussis, A. Kokalj, M. Lazzeri, L. Martin-Samos *et al.*, *J. Phys.: Condens. Matter* **21**, 395502 (2009).
- [25] M. Schlipf and F. Gygi, *Comput. Phys. Commun.* **196**, 36 (2015).
- [26] S. Baroni, S. de Gironcoli, A. Dal Corso, and P. Giannozzi, *Rev. Mod. Phys.* **73**, 515 (2001).
- [27] See Supplemental Material at <http://link.aps.org/supplemental/10.1103/PhysRevB.106.045207> for details about force constant extraction, computational methodology, convergence of results with employed numerical parameters, and mode-dependent phonon properties of all reported materials, which includes Refs. [33–36].
- [28] Note that as presented in Sec. S6, the number of four-phonon processes, i.e., four-phonon scattering, the phase space is nonzero for all modes and is minimally affected by frequency gaps in the phonon spectrum.
- [29] See Sec. S6 in the SM for the relative bonding strength of *s*- vs *p*-block atoms at the *A/B* sites in the considered materials.
- [30] The effective stiffness is obtained by displacing atoms by a small amount (up to 0.1 Å) around their equilibrium positions to sample the effective potential energy surface. Note that this corresponds to an on-site self-harmonic force constant.
- [31] A. F. Ioffe and A. R. Regel, *Progress in Semiconductors*, Vol. 4 (Wiley, New York, 1960).
- [32] The Ioffe-Regel limit is obtained as the minimum interatomic spacing in the lattice.
- [33] D. West and S. Estreicher, *Phys. Rev. Lett.* **96**, 115504 (2006).
- [34] O. Hellman, P. Steneteg, I. A. Abrikosov, and S. I. Simak, *Phys. Rev. B* **87**, 104111 (2013).
- [35] A. Jain, S. P. Ong, G. Hautier, W. Chen, W. D. Richards, S. Dacek, S. Cholia, D. Gunter, D. Skinner, G. Ceder, and K. A. Persson, *APL Mater.* **1**, 011002 (2013).
- [36] C. Kittel, *Introduction to Solid State Physics*, 6th ed. (Wiley, New York, 1986).